

LASER APPLICATIONS AND OTHER TOPICS IN QUANTUM ELECTRONICS

PACS numbers: 07.57.Hm; 42.65.Re
DOI: 10.1070/QE2008v038n11ABEH013888

Generation of terahertz radiation upon filtration of a supercontinuum produced during the propagation of a femtosecond laser pulse in a GaAs crystal

A.O. Vardanyan, D.L. Oganesyan

***Abstract*. The results of a theoretical study of the formation of a supercontinuum produced due to the interaction of femtosecond laser pulses with an isotropic nonlinear medium are presented. The system of nonlinear Maxwell's equations was numerically integrated in time by the finite-difference method. The interaction of mutually orthogonal linearly-polarised 1.98-μm, 30-fs, 30-nJ pulses propagating along the normal to the $\langle 110 \rangle$ plane in a 1-mm-long GaAs crystal was considered. In the nonlinear part of the polarisation medium, the inertialless second-order nonlinear susceptibility was taken into account. The formation process of a terahertz pulse obtained due to the supercontinuum filtration was studied.**

Keywords: *femtosecond laser pulse, terahertz pulse, susceptibility, optical rectification, finite-difference method.*

1. Introduction

A significant advance in generation and detection of coherent pulsed radiation in the frequency region from units to tens of terahertz has been made in the last decade [1 – 3]. Various materials for the generation and detection of terahertz radiation (THR) have been studied. At present, there exist generators of $\sim$ 100-fs pulses with the spectral width of 0.2 – 70 THz whose energy conversion efficiency achieves 10^{-6} [1, 2].

To generate pulsed THR, the optical rectification effect [4] is used, in particular, in nonlinear crystals. Coherent femtosecond THR is detected by using the electrooptical effect in nonlinear crystals [5, 6].

The generation of THR during the interaction of a femtosecond laser pulse (FLP) with a nonlinear isotropic medium is theoretically described by the wave equation in which the time profile of the laser pulse is assumed invariable. It is obvious that this assumption is inacceptable for FLPs, because during the dispersion spreading of a broadband FLP propagating in a nonlinear crystal, both the time profile and the current frequency of the laser pulse change, which, in turn, restricts the crystal length. Upon nonlinear interaction of the FLP with a nonlinear crystal, one can single out from the broad FLP spectrum many pairs of frequency components whose mixing leads to the THR generation. To achieve efficient generation, the group velocity of the optical pulse should be equal to the phase velocity of the terahertz pulse. When the phase matching condition is fulfilled, the fields produced at each point at the crystal output will constructively interfere and the resulting signal will be proportional to the crystal thickness. In this case, to describe the generation of THR propagating in the crystal, it is necessary to take into account the frequency dependence of the crystal refractive index both in the optical and terahertz frequency range.

Terahertz radiation is generated in an isotropic GaAs crystal, which has the transparency band between 0.9 and 17 μm and the absorption coefficient smaller than 5 cm^{-1} in the frequency range up to 3 THz [7]. The nonlinear susceptibility coefficient of the GaAs crystal is rather high and is comparable with these coefficients for such crystals as ZnTe, GaP, GaSe, which are also used to generate THR. Note that the wavelength of the femtosecond laser pump pulse should exceed 1.75 μm, because at this wavelength the GaAs crystal exhibits two-photon absorption. Thus, to generate THR in the GaAs crystal, it is rather promising to use, in particular, fibre lasers emitting femtosecond pulses at 1.98 μm [8].

In this paper, we present the theoretical study of the generation of THR upon filtration of the supercontinuum, which was produced during the FLP propagation in a GaAs crystal. The system of nonlinear Maxwell's equations has been numerically integrated in time by the finite-difference method. The interaction of mutually orthogonal linearly-polarised 1.98-μm, 30-fs, 30-nJ pulses propagating along the normal to the $\langle 110 \rangle$ plane in the 1-mm-long GaAs crystal is considered. It is shown that the regime of stationary THR generation at 16.6 μm takes place in a crystal of this length.

2. Mathematical model describing the nonlinear interaction of mutually orthogonal linearly-polarised FLPs

We will describe the propagation of mutually orthogonal linearly-polarised plane waves along the y axis coinciding with the normal to the $\langle 110 \rangle$ plane of the GaAs crystal by using the system of Maxwell's equations for the electric and magnetic field strengths:

$$\frac{\partial D_z}{\partial t} = -\frac{\partial H_x}{\partial y}, \qquad \frac{\partial D_x}{\partial t} = \frac{\partial H_z}{\partial y},$$

A.O. Vardanyan, D.L. Oganesyan Yerevan Scientific-Research Institute for Optophysical Measurements, ul. Ara Sarkisyana 5a, 375031 Erevan, Armenia; e-mail: yeroptphys@netsys.am

Received 14 May 2008; revision received 5 August 2008
Kvantovaya Elektronika **38** (11) 1070 – 1077 (2008)
Translated by I.A. Ulitkin

$$\frac{\partial H_x}{\partial t} = -\frac{1}{\mu_0}\frac{\partial E_z}{\partial y}, \quad \frac{\partial H_z}{\partial t} = \frac{1}{\mu_0}\frac{\partial E_x}{\partial y}, \tag{1}$$

$$E_z = \frac{D_z - (P_{z\mathrm{L}} + P_{z\mathrm{NL}})}{\varepsilon_0}, \quad E_x = \frac{D_x - (P_{x\mathrm{L}} + P_{x\mathrm{NL}})}{\varepsilon_0},$$

where D_z, D_x are electric inductions; $P_{z\mathrm{L}}$, $P_{x\mathrm{L}}$ and $P_{z\mathrm{NL}}$, $P_{x\mathrm{NL}}$ are the linear and nonlinear parts of the medium polarisation, respectively.

The electric inductions are determined from the constitutive equations, in which the linear dispersion and the nonlinear polarisation of the medium are taken consistently taken into account:

$$D_{z,x} = \varepsilon_0 E_{z,x} + P_{z,x\mathrm{L}} + P_{z,x\mathrm{NL}}. \tag{2}$$

For the selected geometry, the nonlinear polarisation of the medium caused by the nonlinear quadratic susceptibility in the quasistatic approximation can be represented in the from

$$\begin{aligned} P_{z\mathrm{NL}}(t) &= \varepsilon_0 d_{14} E_x^2(t), \\ P_{x\mathrm{NL}}(t) &= \varepsilon_0 d_{14} E_z(t) E_x(t)\sqrt{2}, \end{aligned} \tag{3}$$

where $d_{14} = 150 \times 10^{-12}$ m V^{-1} is the nonlinear susceptibility coefficient of the GaAs crystal. The quasistatic approximation corresponds to the instantaneous nonlinear response of the medium and can be also used in the IR range [9].

As an isotropic nonlinear dispersion medium, the GaAs crystal was used, which is transparent in the spectral region from 0.97 to 17 μm; its linear susceptibility according to [7] can be written in the form

$$\chi^{(1)}(\omega) = n^2(\omega) - 1 = b_0 + \sum_{i=1}^{3} \frac{b_i (2\pi c)^2}{\omega_i^2 - \omega^2}, \tag{4}$$

where $b_0 = 4.372514$; $b_1 = 27.83972$; $b_2 = 0.031764 + 4.35 \times 10^{-5}\Delta T + 4.664 \times 10^{-7}\Delta T^2$; $b_3 = 0.00143636$; $\lambda_1(\mu\mathrm{m}) = 0.4431307 + 0.50564 \times 10^{-4}\Delta T$; $\lambda_2(\mu\mathrm{m}) = 0.8746453 + 0.1913 \times 10^{-3}\Delta T - 4.882 \times 10^{-7}\Delta T^2$; $\lambda_3(\mu\mathrm{m}) = 36.9166 - 0.011622\Delta T$; $\lambda_i = 2\pi c/\omega_i$; ΔT is the temperature deviation from room temperature ($t = 20\,^{\circ}\mathrm{C}$, $T = 293$ K).

According to (4), the linear response of the medium for x and z polarisations is determined by the expressions:

$$P_{x\mathrm{L},z\mathrm{L}}(\omega) = \varepsilon_0 \left[b_0 + \sum_{i=1}^{3} \frac{b_i (2\pi c)^2}{\omega_i^2 - \omega^2} \right] E_{x,z}(\omega)$$

$$= \varepsilon_0 b_0 E_{x,z}(\omega) + P_{1x\mathrm{L},1z\mathrm{L}}(\omega) + P_{2x\mathrm{L},2z\mathrm{L}}(\omega) + P_{3x\mathrm{L},3z\mathrm{L}}(\omega). \tag{5}$$

System of equations (5) can be represented in the form of the system of differential equations

$$\frac{1}{\omega_i^2}\frac{\partial^2 P_{iz\mathrm{L}}}{\partial t^2} + P_{iz\mathrm{L}} = \varepsilon_0 \frac{b_i (2\pi c)^2}{\omega_i^2} E_z(t), \tag{6}$$

$$\frac{1}{\omega_i^2}\frac{\partial^2 P_{ix\mathrm{L}}}{\partial t^2} + P_{ix\mathrm{L}} = \varepsilon_0 \frac{b_i (2\pi c)^2}{\omega_i^2} E_x(t), \tag{7}$$

where $i = 1, 2, 3$.

Expressions (6), (7) describe the linear dispersion properties of the medium in the transparency band in accordance with the classical Lorentz model.

Taking (3) and (5) into account, expressions for the electric inductions D_z and D_x can be presented in the form:

$$D_z = \varepsilon_0 E_z + \varepsilon_0 b_0 E_z + \sum_{i=1}^{3} P_{iz\mathrm{L}} + \varepsilon_0 d_{14} E_x^2, \tag{8}$$

$$D_x = \varepsilon_0 E_x + \varepsilon_0 b_0 E_x + \sum_{i=1}^{3} P_{ix\mathrm{L}} + \sqrt{2}\varepsilon_0 d_{14} E_z E_x. \tag{9}$$

We used the above classical model of interaction of mutually orthogonal polarised FLPs with the anisotropic dispersion nonlinear medium to describe the process of parametric generation of IR radiation [9]. In this paper, this model is adapted for studying the supercontinuum generation produced upon nonlinear interaction of mutually orthogonal polarised FLPs propagating in the GaAs crystal. We considered the case when the carrier frequencies of interacting pulses were the same.

2.1 Numerical scheme of integration of the system of nonlinear Maxwell's equations by the finite-difference method in the time domain

To simulate numerically processes described by expressions (1), (6)–(9), we will pass to the mesh functions for the fields E_z, E_x and H_x, H_z, electric induction D_z, D_x, linear and nonlinear responses $P_{z\mathrm{L}}$, $P_{x\mathrm{L}}$ and $P_{z\mathrm{NL}}$, $P_{x\mathrm{NL}}$ for which the networks in the coordinate $k\Delta y$ and time $n\Delta t$ are specified. The step of the space network Δy was chosen equal to $\lambda_0/300 = 6.6$ nm ($\lambda_0 = 1.98$ μm), where λ_0 is the central wavelength of the pump pulse. The step of the time network was determined by the Courant condition $\Delta t = \Delta y/(2c)$ and is 0.011 fs. We will show below that when this time step is selected, the linear part of the scheme has dispersion maximally close to the Lorentz dispersion of the medium. The difference scheme is an explicit scheme of the second-order accuracy in y. The values of the magnetic field are specified between the network nodes in the y coordinate and at the intermediate layer in time. The numerical integration is performed for the following normalised quantities:

$$\bar{E}_{z,x} = \left(\frac{\varepsilon_0}{\mu_0}\right)^{1/2} E_{z,x}, \quad \bar{D}_{z,x} = \left(\frac{1}{\varepsilon_0\mu_0}\right)^{1/2} D_{z,x}, \quad \bar{H}_{x,z} = H_{x,z},$$

$$\bar{P}_{z\mathrm{L},x\mathrm{L}} = \left(\frac{1}{\varepsilon_0\mu_0}\right)^{1/2} P_{z\mathrm{L},x\mathrm{L}}, \quad \bar{d}_{14} = d_{14}\left(\frac{\mu_0}{\varepsilon_0}\right)^{1/2}. \tag{10}$$

The initial data for the iteration process are the values of E_x, D_x, E_z, D_z at the nth discrete time step and H_z, H_x at the $n - 1/2$ discrete time step.

We used in calculations the numerical scheme similar to that presented in [10] and employed earlier to describe the formation of the IR radiation [11].

2.2 Dispersion properties and the stability of the numerical scheme

The main problem in realisation of the schemes of numerical integration of nonlinear Maxwell's equations is the algorithm stability. It is shown in this section that the realised finite-difference scheme is highly stable and the account for the nonlinearity in the values of the electric field amplitudes of laser pulses and of the nonlinear crystal lengths under study does not lead to the divergence of the numerical scheme.

To study the dispersion properties and the stability of

the numerical scheme used in this paper, we will present the electric and magnetic fields in the form of plane waves with the angular frequency ω and the wave vector k, which propagate along the y axis,

$$E_{z,x}(y,t) = E_{z0,x0}\sin(\omega t - ky),$$
$$H_{z,x}(y,t) = H_{z0,x0}\sin(\omega t - ky). \quad (11)$$

After substituting expressions (11) in difference equations corresponding to expressions (1), (3), (8) and (9), we obtain the dispersion equations determining the dependence between the angular frequency and the wave vector for x- and z-polarised waves:

$$\sin^2\left(\frac{\pi S}{N}\right)^2\left[1 + b_0 + \sum_{i=1}^{3}\frac{cl_i}{2\cos(2\pi S/N) - al_i} + \gamma_{z,x}\right] = S^2\sin^2\frac{k\Delta y}{2}, \quad (12)$$

where $S = c\Delta t/\Delta y$ is the stability factor; $\gamma_z = \bar{d}_{14}\bar{E}_{x0}$; $\gamma_x = \sqrt{2}\,\bar{d}_{14}\bar{E}_{z0}$; $N = \lambda_0/\Delta y$; $cl_i = b_i(2\pi c\Delta t)^2$; $al_i = 2 - (\omega_i\Delta t)^2$. Dispersion equation (12) in the case of the linear and dispersion-free medium and when the condition $\Delta y \ll \lambda_0$ is fulfilled, is reduced to equation $\omega = ck$. In calculations the stability factor S was set equal to 0.5 and $N = 300$. Consider the case corresponding to the linear dispersion medium ($\gamma_{z,x} = 0$), when expression (12) corresponds to the linear dispersion relation $\omega(k)$. The phase velocity obtained by using dispersion relation (12) has the from:

$$v_{\rm num}^{\rm ph}(N) = \frac{\omega}{k_{\rm num}},$$

where

$$k_{\rm num} = \frac{2}{\Delta y}\sin^{-1}\left\{\frac{1}{S}\sin\frac{\pi S}{N} \times\left[1 + b_0 + \sum_{i=1}^{3}\frac{cl_i}{2\cos(2\pi S/N) - al_i} + \gamma_{z,x}\right]^{1/2}\right\}. \quad (13)$$

One can see from (13) that for $\gamma_{z,x} = 0$ and $N = 300$ the ratio of the phase velocity obtained from the numerical scheme to the phase velocity in the continuous medium $v_{\rm phys}^{\rm ph} = c/n(\lambda_0)$ at $\lambda_0 = 1.98$ is $v_{\rm num}^{\rm ph}(N = 300)/v_{\rm phys}^{\rm ph} = 0.9998$. This means that the wave propagation in the continuous medium over a distance of $505\lambda_0 = 1$ mm, which corresponds to $505\lambda_0/\Delta y = 151500$ steps of the space network will correspond to the wave propagation in the discrete medium over a distance of 151469.8 steps of the space network. This, in turn, corresponds to the error in determining the phase velocity obtained from the numerical scheme, $[(151500 - 151469.8)/300]\cdot 360^\circ \approx 35.85^\circ$ or 9.96 %.

When the medium nonlinearity ($\gamma_{z,x} \neq 0$) is taken into account and the amplitudes of mutually orthogonal polarised waves are equal ($E_{x0} = E_{z0} = 25\times10^8$ V m^{-1}), the ratio $v_{\rm num}^{\rm ph}(N = 300)/v_{\rm phys}^{\rm ph}$ is 0.9997. Thus, the wave propagation in the discrete medium over a distance of 151469.8 steps of the space network will correspond to the wave propagation in the continuous medium over a distance of $505\lambda_0 = 1$ mm. This corresponds to the error in determining the phase velocity obtained from the numerical scheme, $[(151500 - 151469.6)/300]\cdot 360^\circ \approx 36.03^\circ$ or 10.01 %.

The group velocity derived by using dispersion relation (12) is

$$v_{\rm num}^{\rm gr}(\omega) = \left(\frac{{\rm d}k_{\rm num}}{{\rm d}\omega}\right)^{-1},$$

where

$$k_{\rm num}(\omega) = \frac{2}{\Delta y}\sin^{-1}\left\{\frac{1}{S}\sin\left(\frac{\omega\Delta t(N)}{2}\right) \times\left[1 + b_0 + \sum_{i=1}^{3}\frac{cl_i}{2\cos[\omega\Delta t(N)] - al_i} + \gamma_{z,x}\right]^{1/2}\right\}. \quad (14)$$

One can see from (14) that for $\gamma_{z,x} = 0$ and $N = 300$, the ratio of the phase velocities is $v_{\rm num}^{\rm gr}(N = 300)/v_{\rm phys}^{\rm gr} = 0.99940$. This means that the wave propagation in the continuous medium over a distance of $505\lambda_0 = 1$ mm for the time $505\lambda_0/v_{\rm phys}^{\rm gr} = 11.4719$ ps corresponds to the wave propagation in the discrete medium over a distance of 1 mm for the time $505\lambda_0/v_{\rm num}^{\rm gr} = 11.4719$ ps + 6.8928 fs. If the nonlinear medium $\gamma_{z,x} \neq 0$) is taken into account and the amplitudes of mutually orthogonal polarised waves are equal ($E_{x0} = E_{z0} = 2.5\times10^8$ V m^{-1}) $v_{\rm num}^{\rm gr}(N = 300)/v_{\rm phys}^{\rm gr} = 0.99939$, and, hence, the group velocity obtained from the numerical scheme is approximately 0.06 % smaller that the group velocity v in the continuous medium. As follows from the presented numerical estimate, for the considered electric field amplitudes of mutually orthogonal polarised waves and the nonlinear crystal length $L = 1$ mm and $N = 300$, the error in determining the phase and group velocities obtained from the numerical scheme virtually coincides, in the case of the nonlinear interaction with the medium, with the error corresponding to the linear interaction.

3. Formation of a terahertz pulse upon filtration of a supercontinuum. Results of the numerical simulation and discussion

We simulated numerically the spectral and temporal characteristics of mutually orthogonal polarised FLPs propagating in the isotropic GaAs crystal under the following initial conditions:

$$E_{z,x}(t, z = 0) = E_{z0,x0}\exp\left(-\frac{t^2}{\tau_0^2}\right)\cos\left(\frac{2\pi c}{\lambda_0}t\right), \quad (15)$$

where $E_{x0} = E_{z0}$ are the initial pulse amplitudes with mutually orthogonal polarisations; $\tau_0 = 30$ fs is the pulse duration; $\lambda_0 = 1.98$ μm. The crystal length is $L = 1$ mm. The maximum values of the pulse amplitudes are $E_{z0,x0}^{\max} = 2.34\times10^8$ V m^{-1}, which corresponds to the electric field strength of the femtosecond pulse of a fibre laser [8] and the path length of the nonlinear conversion $L_{\rm n} = \lambda_0/(2\gamma) \approx 20$ μm.

We estimated the condition of the phase-matching fulfilment by determining the phase coherence length in the case under study, which according to [11] is

$$L_{\rm coh}(\Lambda, \Delta T) = \frac{\pi}{\Delta k(\Lambda, \Delta T)} = \frac{\Lambda}{2[n_{\rm opt}(\lambda_0, \Delta T) - n_{\rm THR}(\Lambda, \Delta T)]}, \quad (16)$$

where $\Delta k(\Lambda, \Delta T)$ is the wave vector detuning; n_{opt} and n_{THR} are the refractive indices in the optical and terahertz regions. When the terahertz radiation wavelength is changed from 4 to 17 μm, the quantity L_{coh} varies from 55 to 68 μm, the maximum value of the phase coherence length being $L_{coh} = 77$ μm and corresponding to the IR radiation wavelength, which is equal to ~ 12 μm. The phase coherence length begins to drastically decrease with increasing the wavelength to 20 μm. Thus, for the crystal length of 77 μm, THR is generated in the absence of the phase-matching condition.

Figure 1 presents the numerical dependence of the normalised duration (at the 1/e level) of mutually orthogonal polarised FLPs on the crystal length. Note that for the initial field strength amplitudes of the FLP and due to the crystal isotropy, the rate of the time spreading of pulses upon changing the crystal length for z- and x-polarised pulses is almost the same. One can see from Fig. 1 that for the crystal length of 100 μm the duration of the laser pump pulse at the crystal output is approximately the same as that at its input. The change in the laser pulse duration in our case is determined by the medium dispersion. In particular, for $L = 1$ mm, the pulse duration at the crystal increases by 3.1 times in our case.

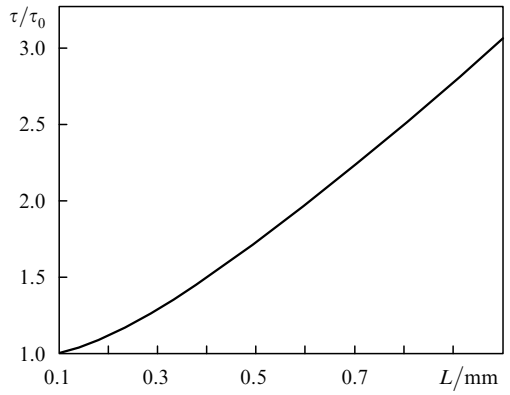

Figure 1. Calculated dependence of the normalised duration of mutually orthogonal polarised laser pulses on the crystal length.

Figure 2 presents the time profiles and spectral power densities for the z-polarised pulse at the crystal input and output; the time profile and the normalised power density at the crystal output

$$S_z\left(\nu = \frac{c}{\lambda}, y = L\right) = 10 \lg \frac{P_z}{P_{z0}}$$

$$= 10 \lg \left(\frac{\left| \int_{-\infty}^{\infty} E_z(t, y = L) \exp(\mathrm{j}\, 2\pi \nu t) \mathrm{d}t \right|^2}{\left| \int_{-\infty}^{\infty} E_z(t, y = 0) \exp(\mathrm{j}\, 2\pi \nu t) \mathrm{d}t \right|^2} \right) \qquad (17)$$

were obtained in numerical calculations for $E_{z0} = E_{z0,\,x0}^{max}$ and $L = 1$ mm. The laser pulse duration at the output of the nonlinear crystal, according to Figs 1 and 2c is ~ 93 fs. One can see from Fig. 2d that the supercontinuum distribution is produced at the crystal output in the FLP spectrum in the region of difference frequencies; it also shows the spectral window in the frequency range from 10 to 70 THz, which is responsible for filtration. Note that upon filtering by this idealised mathematic filter the phase ratio between the spectral components in the difference frequency region within the filter transmission band remains the same as that, which is produced during the pulse propagation in the crystal. Bandpass filters in the spectral region from 4.28 to 30 μm can be realised based on multilayer dielectric filters [12, 13]. It is obvious that when real filters are used the phase ratio between spectral

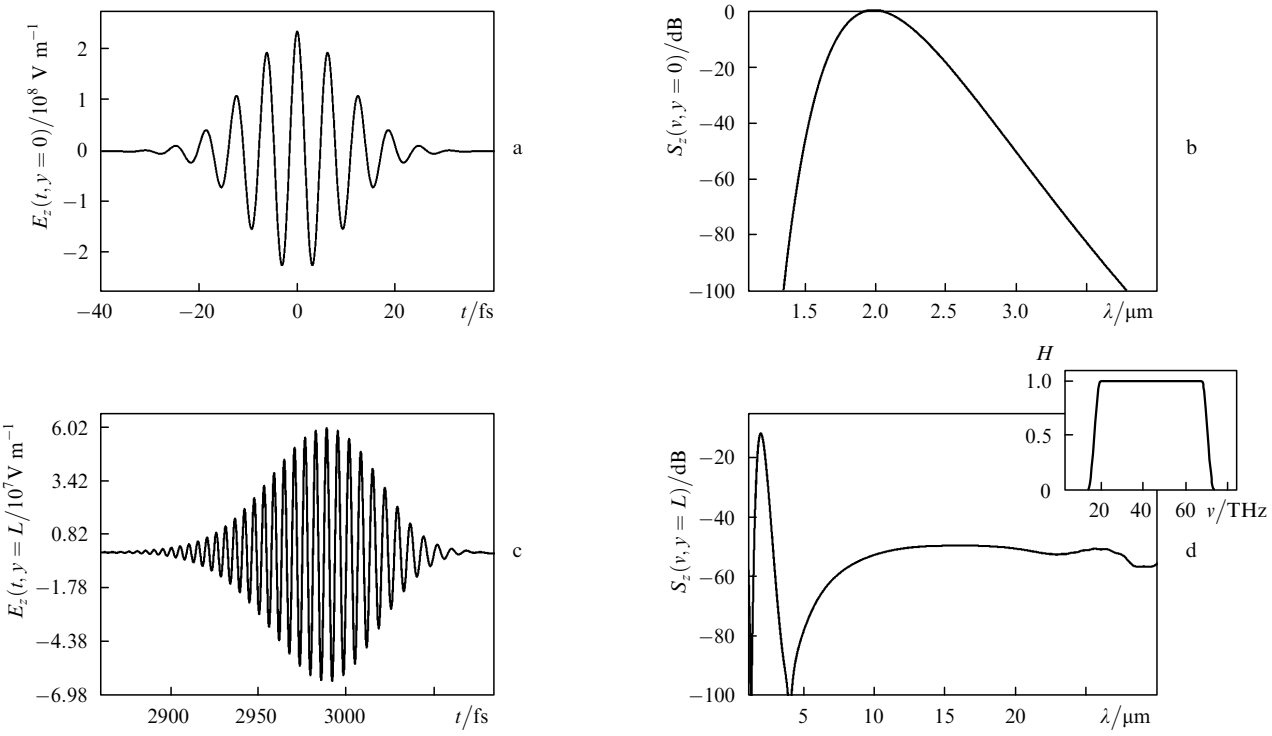

Figure 2. Time profiles (a, c) and wavelength dependences of the power density (b, d) for the z-polarised pulse at the crystal input (a, b) and output (c, d) as well as the spectral window in the frequency range from 10 to 70 THz, which is responsible for filtration of the produced supercontinuum (d).

components in the difference frequency region falling in its passband will be determined also by the phase–frequency characteristic of the filter. To separate the visible and near-IR spectra from the frequency range under study, it is necessary to preliminary transmit the pulses from the nonlinear crystal output through a silicon or germanium filter [14].

Figure 3 presents the time profiles and frequency dependences of the THR power densities obtained due to filtration of the supercontinuum for different crystal lengths.

Figure 4 shows the time dependences of the normalised current frequency for the z-polarised pump pulse

$$\bar{\omega}(t) = \frac{\omega_0 - \omega(t)}{\omega_0}, \quad \omega_0 = \frac{2\pi c}{\lambda_0} \tag{18}$$

and normalised current THR frequency

$$\bar{\Omega}(t) = \frac{\Omega(t) - \Omega_{0\max}}{\Omega_{0\max}}, \quad \Omega_{0\max} = \frac{2\pi c}{\Lambda_{0\max}} \tag{19}$$

for different lengths of the nonlinear crystal. Here, $\Lambda_{0\max}$ is the wavelength corresponding to the maximum of the spectral distribution in the filtered supercontinuum.

One can see from Figs 3b and 4b that for the crystal lengths 100, 400, 700, 850 μm and 1 mm the maximum of the spectral distribution in the filtered supercontinuum falls at the terahertz radiation frequency of ~ 19 THZ (15.8 μm) and for the crystal lengths 250 and 550 μm – at frequencies of ~ 32 THz (9.4 μm) and ~ 23.4 THz (12.79 μm).

According to Fig. 4a, the laser pulse, apart from the temporal dispersion spreading, acquired also frequency modulation (positive chirp) due to which long wavelength components start to outrun the short wavelength components (which corresponds to the region of the normal dispersion of the medium). According to Fig. 4a, the current frequency for the z-polarised pump pulse linearly depends on the time as

$$\omega(t) = \omega_0 - 2\alpha t. \tag{20}$$

Figure 5 shows the dependence of the chirp $\alpha\tau^2$ ($\tau = \tau_0 2\sqrt{\ln 2}$) on the crystal length. According to the calculations, during its propagation in the crystal, the transform-limited laser pulse (15) is transformed in a pulse with a linear frequency modulation, whose sign is determined by the medium dispersion [15].

It follows from the above that if a laser pump pulse with

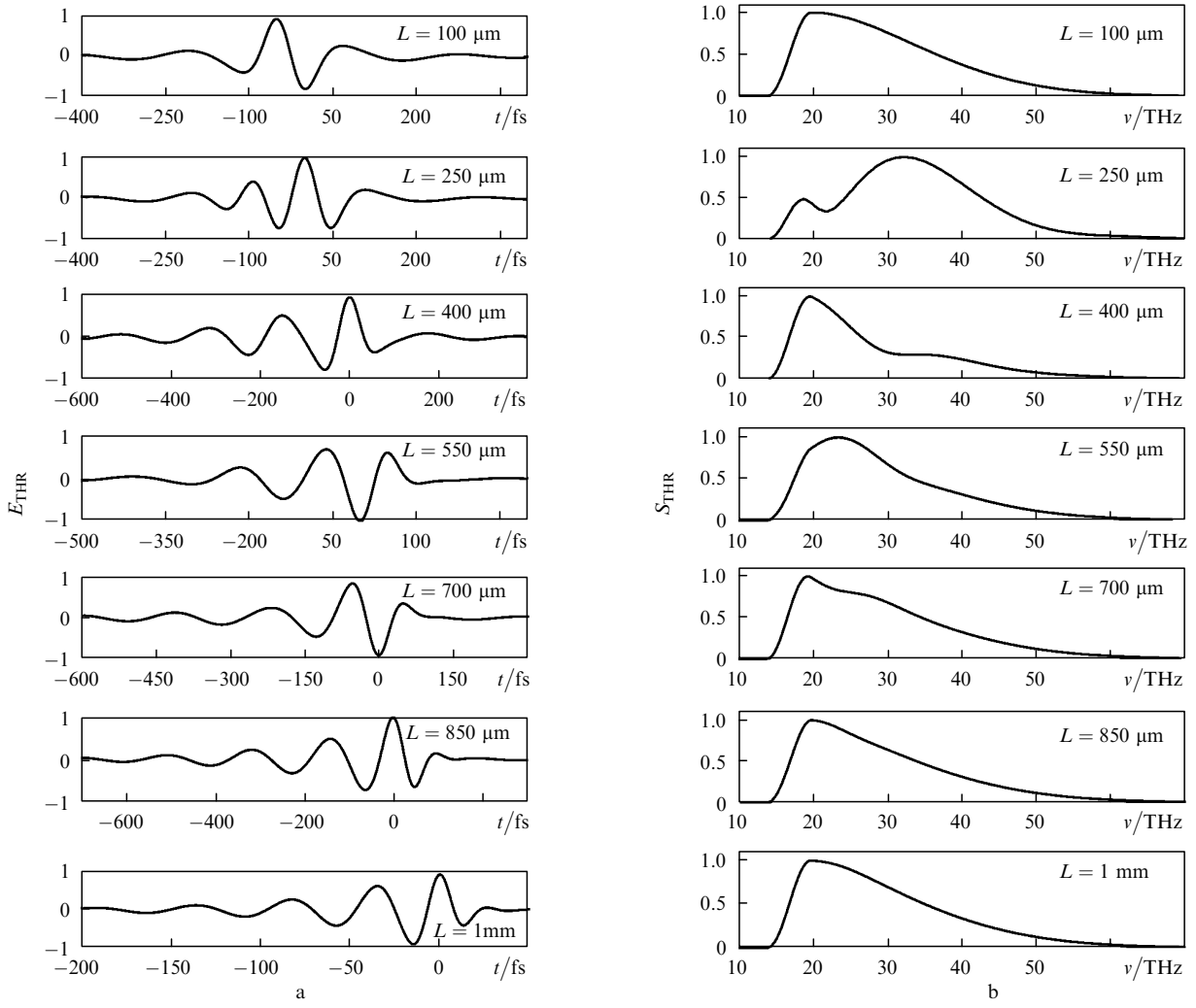

Figure 3. Time profiles (a) and frequency dependences of the power density of terahertz radiation (b) obtained upon filtration of the spectral supercontinuum produced upon propagation of the z-polarised pulse in the crystal of different lengths L.

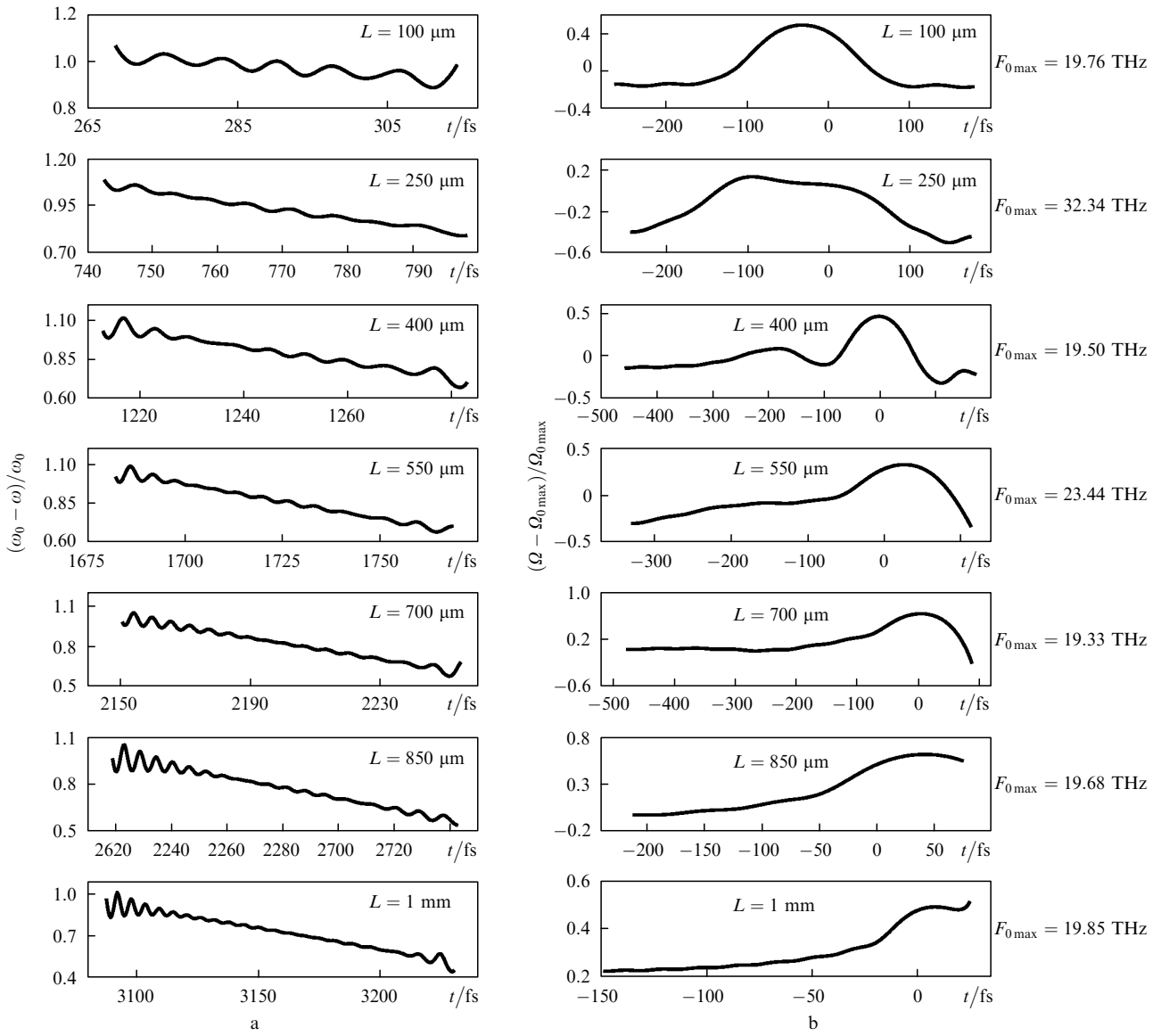

Figure 4. Time dependences of the normalised current frequency for the z-polarised pump pulse (a) and normalised current THR frequency (b) for different values of L.

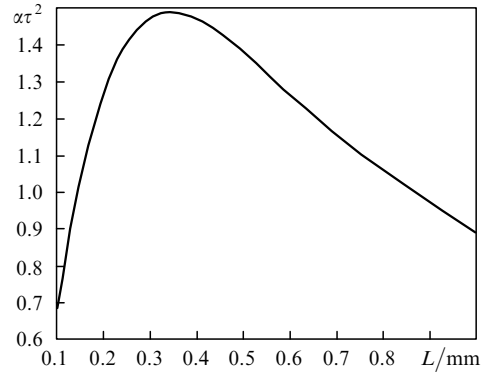

Figure 5. Dependence of the pump pulse chirp $\alpha\tau^2$ on the crystal length.

a negative chirp is produced and the chirp value is chosen in accordance with the dependence $\alpha(y)$ shown in Fig. 5 and the pulse duration $\tau(y)$ – in accordance with the dependence presented in Fig. 1, the pulse duration at the crystal output will be determined by the full width of the spectrum τ_0 and the rate of the frequency change will be equal to zero. This, in turn, will lead to an increase in the generation efficiency of terahertz radiation with the high-frequency spectral components at the output of the nonlinear crystal.

Figure 6 presents the dependences of the normalised pump density of THR obtained upon filtration of x- and z-polarised laser pulses on the crystal length for the initial values of the field strengths $E_{x0} = E_{z0} = 234$ and 135 MV m^{-1}. According to Fig. 6, the conversion efficiency for the x-polarised pulse is 5 dB lower than that for the z-polarised pulse, which is determined by the selected geometry of the problem [see (8) and (9)].

The curves presented in Fig. 6 correspond to the dependence of the THR generation efficiency on the crystal length obtained in the slowly-varying amplitude approximation, which for picosecond and subpicosecond pulses has the form:

$$S_{\mathrm{THR}}(\Omega, y) \sim \sin c^2\left[\left(\Delta u^{-1}\Omega - \Delta k(\Lambda, \Delta T)\right)\frac{y}{2}\right], \qquad (21)$$

where

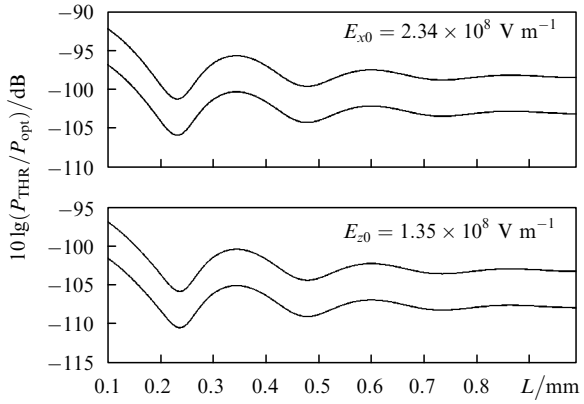

Figure 6. Dependences of the normalised power density of terahertz radiation obtained upon filtration of x- and z-polarised laser pulses on the crystal length for the initial field strengths $E_{x0} = E_{z0} = 2.34 \times 10^8$ and 1.35×10^8 V m^{-1}.

$$\Delta u^{-1} = \left(\left. \frac{\partial k_{THR}}{\partial \omega} \right|_{\omega=\omega_{THR}} - \frac{\partial k_0}{\partial \omega} \right)^{-1}$$

is the group velocity detuning.

The length of the group delay, determined by the group velocity detuning, is

$$L_{gr}(\omega) = \frac{2\pi}{\Delta\omega} \Delta u^{-1}, \quad (22)$$

where the spectral width of the laser pump pulse $\Delta\omega$ mainly determines the nonlinear interaction. When the THR wavelength is changed from 4 to 16.6 μm, L_{gr} varies from 198 to 1050 μm. Thus, for the 1-mm-long crystal, the regime of the stationary THR generation at 16.6 μm takes place.

Figure 7 presents the numerical dependence of the normalised power density of the x- and z-polarised THR on the pump pulse energy

$$10\lg\frac{P_{THR}}{P_{opt}} = 10\lg\left(\frac{\left| \int_{\nu_1}^{\nu_2} E_{x,z}(\nu, y = L) H(\nu) \mathrm{d}\nu \right|^2}{\left| \int_0^{\infty} E_{x,z}(\nu, y = L) \mathrm{d}\nu \right|^2} \right) \quad (23)$$

for the crystal lengths $L = 100$ μm and 1 mm and the equality of the strengths E_x and E_z of laser pulses. In expression (23), the frequencies $\nu_1 = 10$ THz (30 μm), $\nu_2 = 70$ THz (4.28 μm) correspond to the frequency interval in which spectral filtration is performed.

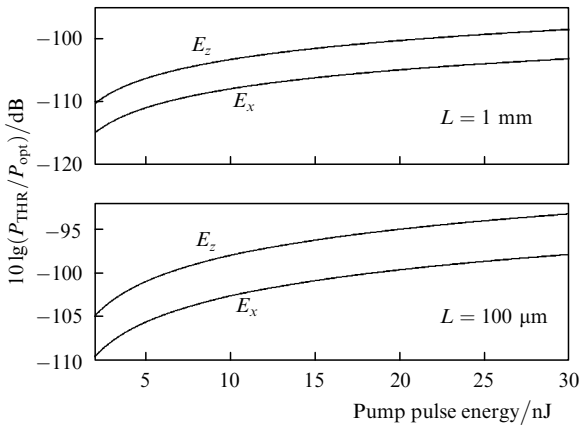

Figure 7. Calculated dependences of the normalised power density of x- and z-polarised THR on the pump pulse energy for $L = 1$ mm and 100 μm.

These curves correspond to the dependence $|E_{THR}|^2 \sim |E_{opt}|^4$ presented in the logarithmic scale. One can see from the results of calculations and Fig. 7 that for $L = 1$ mm the maximum conversion efficiency for the z-polarised wave is −98 dB and for the x-polarised wave it is −103 dB; for $L = 100$ μm, the maximum conversion efficiency for these waves is −93 and −98 dB, respectively. In this case, the THR generation efficiency is 5 dB higher for $L = 100$ μm than that for $L = 1$ mm. This is mainly determined by the fact that for $L = 100$ μm the pump pulse duration coincides with the pulse duration at the crystal input.

4. Conclusions

We have performed the theoretical study of the generation of THR obtained upon filtration of a supercontinuum produced during the propagation of femtosecond laser pulses in a GaAs crystal. The system of nonlinear Maxwell's equations has been numerically integrated in time by the finite-difference method. The interaction of mutually orthogonal linearly-polarised 1.98-μm, 30-fs, 30-nJ FLPs, which propagate along the normal to the ⟨110⟩ plane in the 1-mm-long GaAs crystal, has been considered. In the nonlinear part of the medium polarisation, the inertialless nonlinear second-order susceptibility has been taken into account. It has been shown that to increase the THR generation efficiency during the FLP propagation in the GaAs crystal of length L, it is necessary to produce a laser pump pulse with the negative chirp in accordance with the dependence $\alpha(y = L)$ (Fig. 5) and the pulse duration in accordance with the dependence $\tau(y)$ (Fig. 1). Indeed, when this FLP propagates in the GaAs crystal of length L, its duration at the output will be determined by the spectrum full width and the rate of change in the frequency modulation will become equal to zero. This, in turn, will lead to the increase in the generation efficiency of terahertz radiation with the high-frequency spectral components at the output. The time dependences of the current frequency and pump pulse duration as well as of the current THR frequency have been obtained for different crystal lengths. The dependences of the THR generation efficiency on the crystal length and the pump pulse energy have been presented. It has been shown that for the 100-μm-long crystal the maximum conversion efficiency for the z-polarised wave is −93 dB and for the x-polarised wave it is equal to −98 dB.

The results obtained in this paper can be used, in particular, to develop pulsed terahertz sources.

References

1. Grischowsky D., Keiding S., van Exter M., Fattinger Ch. *J. Opt. Soc. Am. B*, **7**, 2006 (1990).
2. Mittleman D.M., Gupta M., Neelmani R., et. al. *Appl. Phys. B*, **10**, 1007 (1999).
3. Chen Q., Zhang X.-C. *Phys. Lett.*, **74**, 3435 (1999).
4. Ding Y., Zotova I. *Opt. Quantum Electron.*, **32**, 531 (2000).
5. Wu Q., Zang X.-C. *Appl. Phys. Lett.*, **67**, 3523 (1995).
6. Chaltikyan V.O., Hovhannisyan D.L., Laziev E.M., Melikyan A.O., Vardanyan A.O. *J. Modern Opt.*, **53** (7/10), 919 (2006).

7. Skauli T., Kuo P.S., Vodopyanov K.L., Pinguet T.J., Levi O., Eyres L.A., Harris J.S., Fejer M.M., Ginzton E.L., Gerard B., Becouarn L., Lallier E. *J. Appl. Phys.*, **94** (10), 6447 (2003).
8. Imeshev G., Fermann M.E., Vodopyanov K.L., Fejer M.M., Ginzton E.L., Yu X., Harris J.S. *Opt. Express*, **14** (10), 4439 (2006).
9. Hovhannisyan D.L, Stepanyan K.G., Avagyan R.A. *Opt. Commun.*, **245**, 443 (2005).
10. Fujii M., Tahara M., Sakagami I., Freude W., Russer P. *IEEE J. Quantum Electron.*, **40** (2), 175 (2004).
11. Hovhannisyan D.L., Vardanyan A.O. *J. Lasers Engineering*, **8**, (1-2), 35 (2008).
12. Holah G.D. *Far-Infrared and Submillimeter-Wavelength Filters, in Infrared and Millimeter Waves*. Ed. by K.J. Button (NY.: Acad. Press, 1982) Vol. 6, p. 305.
13. Hawkins G.J., Hunneman R., Gardner M.T., Babcock G.T. *Infrared Phys. & Technol.*, **39**, 297 (1998).
14. Zentgraf T., Huber R., Nielsen N.C., Chemla D.S., Kaindl R.A. *Opt. Express*, **15** (9), 5775 (2007).
15. Akhmanov S.A., Vysloukh V.A., Chirkin A.S. *Optics of Femtosecond Laser Pulses* (New York: AIP, 1992; Moscow: Nauka, 1988).